Soil Salinity Induced Land Cover Change Detection and Analysis in Siwa Region, NW Egypt.

Alaa A. MASOUD[1, 2] **and Katsuaki KOIKE**[1]

[1] Department of Civil and Environmental Engineering, Faculty of Engineering, Kumamoto University, 2-39-1 Kurokami, Kumamoto 860-8555, Japan.
[2] Corresponding author's e-mail:alaa2004@gpo.kumamoto-u.ac.jp.

ABSTRACT

Siwa region located north in the Western Desert of Egypt has been recently subjected to severe soil salinity problems. Monitoring and analysis of the recent land cover dynamics integrating remote sensing and GIS could provide base information to document salinity change trends and anticipate further degradation where the absence of long-term salinity records is an obstacle. Three Landsat TM/ETM+ satellite images over a span of 16 years (1987-2003) coupled with a 30-m DEM and field observations served as the basic source of data. Standard image enhancements, classification, and change detection techniques were applied to determine changes between the available images. Changes were analyzed in integration with land surface characteristics such as slope, radiometric thermal temperature, vegetation indices, and tassel cap transformations. Such analysis enabled characterizing the alteration in vegetation cover and provided the evidences to locate possible future changes due to soil salinity. Results showed acceleration in the rate of soil salinization and vegetation clear-cuts after the year 2000. Recommendations and measures that may prevent or ameliorate the exacerbation of the problem are called for.

1. INTRODUCTION

Siwa region has recently been a drastic example of the Egyptian lands experiencing severe soil salinity conditions that had lead to many serious environmental and socio-economic problems. A significant reduction in the area of the productive land cultivated with date palms and olive trees has recently taken place. Remedial actions require reliable information to help set priorities and to choose the type of action that is most appropriate to combat the problem. Unfortunately, no salinity records exist that could enable to establish long-term salinity trends and to date, there is no knowledge base for identifying areas at potential risk to salinity. Reliable and up-to-date information on the recent changes of the land cover dynamics, in particular, shifts in the vegetation cover and extent of the salt marshes could help provide base information to document salinity change and anticipate further degradation. The integrated use of satellite remote sensing and Geographic Information System (GIS) in such ecologically sensitive region is well suited. Such integration has been determined to be a powerful and cost-effective approach, however, results to date indicate that no uniform combination of data type and analytical method can be applied with equal success across broadly variable ecosystem conditions (Lunetta et al., 2002; Zhan et al., 2002).

The primary emphasize of this paper is to monitor land cover patterns and to detect changes occurred over a span of 16 years (1987–2003) in the region. Shifts in the vegetation cover and the extent of the salt marshes will be analyzed and characterized to locate possible near future clear-cuts in the date palms and the olive trees. In the following sections, the study area is introduced, data used and the preprocessing steps are explained, image processing and GIS analysis for temporal land cover mapping and characterization as well as

change detection and locating possible future changes methods are described. Finally, results are shown, conclusions are drawn and recommendations are called for.

2. STUDY AREA

The study area covers about 7333 km^2 located Northwest of the Egyptian Western Desert near from the Libyan–Egyptian border and some 300 km to the south from Mersa Matruh on the Mediterranean Sea and 600 km to the west from Cairo (Fig. 1). The climate exhibits extreme aridity with very low rainfall (average of 9.6 mm year^{-1}), high evaporation (17 mm day^{-1} in July to 5.2 mm day^{-1} in December) and high summer temperature (maximum 37.7°C in July). The geomorphology of the area is varied. Three distinctive units are distinguished; the northerly bounding limestone plateau and the steep escarpment running E-W, areas of mobile sand dunes to the south; and closed flat depressions with cultivated land, playas, and saline lakes, whose lowest point is 19 m below sea level. Agriculture developments depend on irrigation supplemented by naturally flowing springs of good quality groundwater resources. These springs have created a network of oases surrounding lakes, named from West eastwardly as: Maraqi, Siwa, Zaitun, and Massir, of which Siwa is the largest and the highly urbanized oasis.

Natural and human-induced factors such as land use mis-management, inadequate drainage system intertwined with the overuse of irrigation water coupled with the presence of saline lakes, high salt content in the underlying old marine sediments, dominance of heavy textured saline soils, severe environment and uncertainly of rainfall, all these factors, either individually or in combination with other factors, has resulted in hydrological imbalance causing the water table to rise in the topsoil. According to Misak et al. (1997), in 1962-1977 the rate of rise was 1.33 cm year^{-1} while in 1977-1990 it measured 4.6 cm year^{-1}. Now, the water table has reached the ground surface in some areas causing advanced stage of salinization that limited the soil resource base. Consequently, extensive patches have been gradually converted into salt marshes.

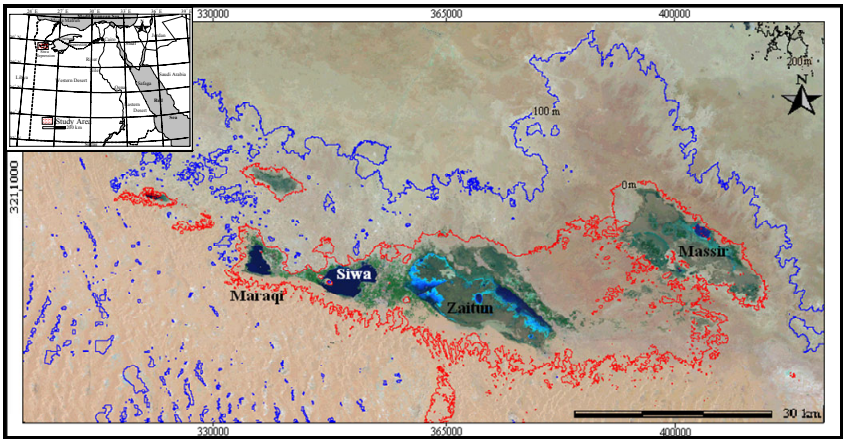

Figure1. Location map of the study area generated from the RGB false color composite of the 2003 ETM+$_{742}$ overlain by contour lines.

3. MATERIALS AND PREPROCESSING

The principal data utilized in this research are, three Landsat data sets (Row 40/Path 180 of the WRS-2); two ETM+ images dated 6 October 2000 and 23 May 2003, and a TM image acquired on 4 November 1987, Shuttle Radar Topographic Mission (SRTM) 30-m

DEM, and field observations collected in October, 2003 including the ground-truth information required for validating the classification and the prediction techniques adopted. The Landsat scenes were acquired under clear atmospheric conditions during the dry season where salt surface features are enhanced and the impact of soil salinity on surface attributes is intensified. These data are geo-referenced to UTM coordinate system, Zone 35 North based on 1:50,000 scale topographic maps with 7.8 m, 9.1 m, 12.2 m, and 12.0 m root mean square error for 2003, 2000, 1987, and the DEM, respectively. The geo-referenced data were then clipped to the study area of 7333 km^2. The radiometric resolution of all the data was adjusted through contrast stretching to 8 bit with 256 levels of brightness. This was carried out on GRASS GIS (GRASS Development Team, 2004) running under windows using CYGWIN.

4. DATA PROCESSING

4.1. Temporal land cover classification and mapping

Several standard image enhancement techniques are applied, following, unsupervised ISODATA clustering was performed on the 2003 image and nine cover classes were spectrally separable. Class boundaries were adjusted through visual inspection and field observations and these classes are used to train the maximum likelihood classifier. Checking the classification performance indicated mis-classification of the flat depression habitats mainly the dry sabkha marshes and wet marshes with salt crusts due to their spectral inhomogeneity. This was also so difficult to separate in the field. The first component of the principal component analysis as well as the panchromatic band was injected to the classifier and classification was re-run. The total and the individual accuracies of the classes were enhanced. The panchromatic band has enhanced the minor features due to its relatively high spatial resolution of 15 m when used separately and fused with the principal component. Further, spatial filtering, injection of the TM/ETM_{531} (red, green, and blue) color composite selected based on optimum index factor (OIF) of Chaves et al. 1982, and feeding the classifier with the wetness index of the tassel cap transformations has considerably enhanced the total and the individual accuracies of the detected classes. The classification accuracies were evaluated at each level of improvement using Kappa coefficients (Congalton, 1991). Also, several image processing techniques to enhance the classification accuracy were investigated such as band rationing, and injection of other indices derived from the image analysis described later including tassel cap transformations, vegetation indices, land surface temperature, did not improve the accuracy much higher than achieved (Table 1).

Table 1: Accuracy assessment of the classified data using Kappa coefficients.

Class \ Data	2003[a]	2003[b]	2000	1987
Water bodies	0.75	0.99	0.99	0.99
Wet sabkha-salt crusts	0.76	0.96	0.95	0.93
Dry Sabkha	0.22	0.90	0.89	0.87
Vegetation	0.89	0.99	0.98	0.99
Sand dunes	0.89	0.93	0.87	0.87
Limestone	0.43	0.67	0.61	0.64
Marl	0.70	0.87	0.85	0.67
Carbonate soil	0.44	0.69	0.64	0.62
Marly soil	0.50	0.79	0.74	0.77
Total Kappa/Correct%	0.56/67.64	0.86/91.62	0.83/89.39	0.81/87.45

2003[a] includes 2003 ETM+ original bands excluding the panchromatic and the thermal bands, and 2003[b] include the original bands as well as the panchromatic band and also several enhanced bands described above.

Classified image was sieved, clumped and filtered before producing final land cover map. Followed a successful classification of 2003 image, 2000 and 1987 data have been classified taking the training classes from the 2003 land cover map following the same classification steps. Three thematic land cover maps were produced (Fig. 2) and their classification accuracies represented by kappa coefficients are shown on Table 1.

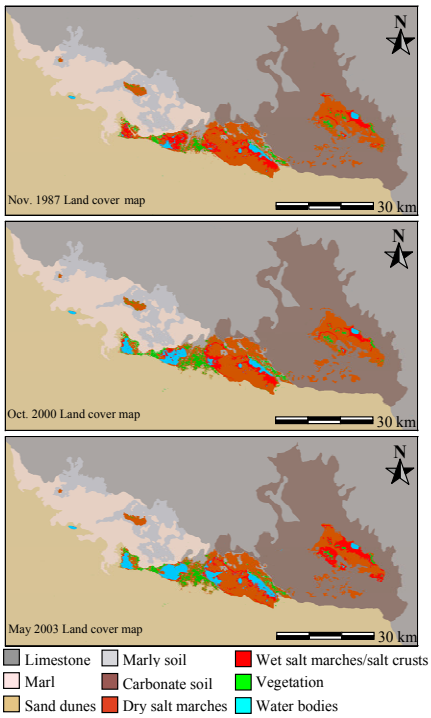

Figure 2. Land cover maps of 1987, 2000, and 2003 of the study area.

4.2. Derivation of the land surface characteristics

Following successful spatio-temporal land cover mapping, various land surface characteristics that may be related to soil salinity were derived, such as the slope, land surface temperature (LST), Soil Adjusted Vegetation Index (SAVI), and the tassel cap transformations. Slope was derived from the topographic analysis of the DEM applying the *r.slope.aspect* module in GRASS GIS on the 30 m SRTM DEM. The soil adjusted vegetation index (SAVI) of Huete, 1988, was applied as follows:

$$\text{SAVI}=\frac{(\rho_{\text{NIR}}-\rho_{\text{red}})}{(\rho_{\text{NIR}}+\rho_{\text{red}}+L)(1+L)} \quad (1)$$

Where ρ is the digital number of the band and L is an adjustment parameter based on the nonlinear extinction of red and NIR through the landscape, and is assumed to be 0.5 for a wide variety of vegetations (Huete, 1988).

Two principal axes of the tassel cap transformations (Kauth and Thomas, 1976) were used; the greenness discriminating vegetated areas and the wetness of the land surface that is sensitive to both soil and vegetation moisture. Due to the spectral similarities between the TM and the ETM+ sensors, the indices can be extracted from TM and ETM+ data using the same coefficients (Huang et al., 2002) as follow:

$$\textit{Greeness} = -0.2728\,B_1-0.2174\,B_2-0.5508\,B_3+0.7221\,B_4+0.0733\,B_5-0.1648\,B_7,$$
$$\textit{Wetness} = 0.1446\,B_1+0.1761\,B_2+0.3322\,B_3+0.3396\,B_4-0.6210\,B_5-0.4189B_7 \quad (2)$$

Where B_i corresponds to the TM/ETM+ spectral band *i*. The wetness index was used in enhancing the classification accuracy of the maximum likelihood classifier as previously mentioned. This index proved well in differentiating between dry sabkha marshes and the wet sabkhas with salt crusts. The greenness will be used in the change detection and analysis task.

To derive the land surface temperatures, the thermal bands of the landsat TM/ETM+ data have been used. Digital numbers (DNs) of these bands were firstly converted to physical measurements of at-sensor radiance (Landsat Project Science Office, 2002) and then transformed into radiant surface temperature values using thermal calibration constants for the TM supplied by Markham and Barker (1986) and for the ETM+ by the Landsat Project Science Office, 2002 as follows:

$$T_s = \frac{K_2}{\ln\left(\frac{K_1}{L_\lambda} + 1\right)} - 273.15 \qquad (3)$$

where T_s is the radiant surface temperature (C°), K_1 and K_2, the pre-launch calibration constants that are, 607.76 and 1260.56 for TM and 666.09 and 1282.71 mW cm^{-2} sr^{-1} μm^{-1} for ETM+, respectively, and the 273.15 is the constant to convert from Kelvin to Celsius temperature degrees. The temperature values obtained above are referenced to a black body. According to Wukelic et al. (1989) and Washburne (1994), the satellite temperatures derived from the Landsat thermal band data give good approximations, within 1–3°C, of the ground temperature values on clear days. They clearly indicate that using inaccurate atmospheric profiles for a possible atmospheric correction could lead to larger error. Due to the lack of local reference atmospheric data and the sky was clear during data acquisition we did not apply any atmospheric corrections. A normalization approach based on the maximum and the minimum values of the SAVI, temperature, and greeness was applied to allow for different date comparison.

4.3. Change detection and analysis

Land cover maps for 1987, 2000 and 2003, were overlaid two at a time and subsequent GIS analyses was performed applying simple image differencing. Land salinized as well as clear-cuts in the vegetation cover occurred after 1987 and 2000 were detected and quantified. Alterations in the vegetation condition depicted by SAVI, surface temperature, and greenness was considered and analyzed for the vegetative areas retained in 1987-2003 period. Changes in slope and surface temperature in particular for the highly dynamic land covers were identified. Analysis of these characteristics indicated that the flat nature of the depression and the continual climate warming suggests that such areas will be worsened and the soil salinity problems will be exacerbated if not efficient management practices to be timely undertaken. Removal of vegetation cover significantly increases the soil moisture content due to reduced evapo-transpiration that consequently raises the shallow water table. Also, density of vegetation cover is of significant importance in governing the rate of evapo-transpiration. The peripheries of the dense vegetation have high rate of evapo-transpiration and hence are at-risk for dryness and this is evident in Siwa.

4.4. Methodology for locating possible future vegetation clear-cuts

Soil salinity is the main cause of alteration for the date palms and the olive trees in Siwa. Analysis of the derived characteristics in the vegetated areas present since 1987 indicated gradual declination for the SAVI, increase in temperature, while the greenness showed slight increase in 2000 and decrease in 2003. Also it was noted that the clear-cut in vegetation was active in areas having lowest slope, the highest surface temperature, and the

lowest SAVI values. Based on these findings, the slope, the temperature, and SAVI of the vegetation cover was thresholded and used to demarcate possible future dryness or clear-cutting based on the likelihood of occurrence. The clear-cuts of the agriculture detected in 2000 and 2003 were cross-tabulated with the land surface maps of the 1987 and 2000, respectively. Average values of the deleted vegetation characteristics are then used as thresholds to locate areas on the next date having characteristic values equal or greater than these thresholds. Deleted vegetation in 2003 was used to detect possible cuts in the near future and clear-cuts in 2000 are used to quantify and validate cuts in 2003. Bolean algebra was applied based on "if-then" rules in GRASS GIS to locate areas having the defined thresholds. Table 2 shows the average values of vegetation condition deleted in year 2000 and 2003 and the predicted areas applying this technique. The technique applied did not give time line for the predicted alteration, but clear-cuts are possibly like to occur if the same conditions will continue to prevail in the near future such as increase in soil salinity, temperature due to global warming phenomenon and in turn dryness of the agriculture.

Table 2: Average clear-cut vegetation condition in 2000 and 2003 as well as the predicted clear-cut average characteristics.

Rank	**Slope (°)**	**Temp. (C°)**	**SAVI**
Vegetation clear –cut 2000	0.64	28.43	8.21
Vegetation clear –cut 2003	0.66	30.16	3.88
Predicted vegetation clear-cut	0.67	31.84	8.6

5. RESULTS AND DISCUSION

Change detection results for Siwa show major changes that include increase in the areal extent of the lake waters and the wet sabkhas and reduction in dry sabkhas and vegetation covers. Where the total coverage of the dry sabkha was lowered due to invasion of the lake waters, a considerable extension of the sabkha was vivid near the vegetation cover and the urban centers. About 47.96 km^2 of the land has been salinized in the period 1987-2000 and about 37.37 km^2 in 2000-2003. These indicate that the salinization rate has been accelerated after the year 2000. An increase in the clear-cut areas of the natural vegetation including the date palms and the olive trees was clear and was of high rate where about 12.63 km^2 has been removed between 2000 and 2003, and 7.8 km^2 has been cut in1987-2000.

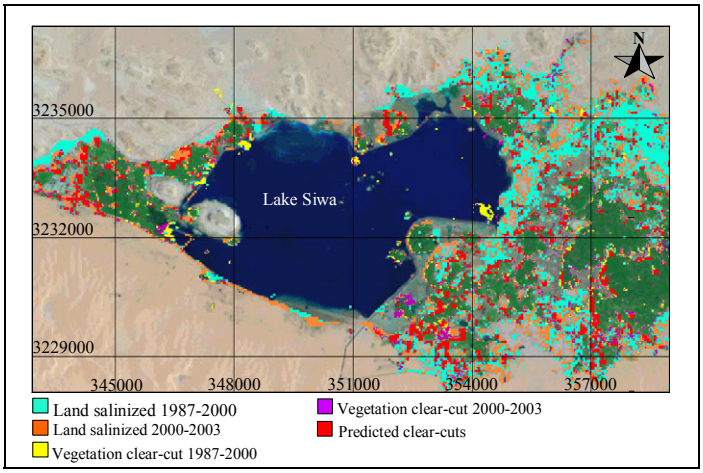

Figure 3. The detected salinized lands and vegetation clear-cuts as well as the areas predicted to be removed in the near future surrounding Lake Siwa.

Most of these areas are located in direct contact with the saline lake waters, the wet sabkhas, or near from urban centers where the effect of the urban heat island is relatively high enhancing the evapo-transpiration rate of the nearby vegetation. Evidenced by the characteristics of the past removed vegetation, 13.81 km2 of the 2003 vegetation cover was predicted to be altered in the near future. Thresholds applied to the year 2000 data provided 18 km^2 of removal that is greater than the deleted areas detected in 2003. This difference may be due to changes in the vegetation condition occurred in the relatively long period of monitoring from 1987 to 2000. The spatial distribution of the salinized lands and the vegetation clear-cuts detected in 2000 and 2003 as well as areas predicted to be removed in the near future surrounding Lake Siwa are shown on Fig. 3.

Field checking in some vegetation localities predicted to be deleted in the area showed that dryness of leaves of the date palms and the olive trees are strongly acting. Also, salt crusts have been noticed in the vicinity of these areas indicating an advanced stage of salinization (Fig. 4).

Figure 4. Photograph showing the salinized soil and vegetation death in Siwa.

6. CONCLUSION

At the most basic level, this work has succeeded in mapping and characterizing the spatio-temporal land cover distribution in Siwa and in identifying the major changes took place over 16 years (1987-2003). Difficulties are imposed by the highly dynamic nature of the land covers, and by the difficulty of obtaining accurate official data on land cover even where such data exist. This problem was approached by combining a conventional multispectral analysis of satellite imagery with data on recent and historical land use gathered through field campaigns. Changes in distribution of the salt marshes and shifts in the vegetation cover have been detected and quantified. Also, near future alterations in the vegetation cover that are most likely to occur were predicted using the only available data. Although time line was not given, the predicted alteration of the vegetation is expected to occur if the present conditions will continue prevailing within the next few years. Such base information can help decision-makers and land planners in the process of determining priority areas for the implementation of salinity action plans or soil reclamation measures at regional level to avoid adverse environmental effects.

Measures based on the findings from this research can be preventive reducing the inflow into the lakes, subsoil, and the shallow water table or ameliorative envisaging the removal of the excess water from the subsoil and to restore the condition conducive for normal growth of vegetation. These measures could include 1) Installation of an appropriate surface and subsurface drainage system, 2) Economical use of water and full utilization of the naturally flowing water in irrigation and other industrial projects in the area, 3) Pumping from subsoil to lower water table, and 4) Bio-drainage by cultivating salt-tolerant trees and

shrubs that have high moisture use and high rate of evapo-transpiration that may serve the triple goal as a natural drainage system, reducing the heat island effect, and in fixing the sand dunes preventing its further encroachment to the area.

Further research could investigate integration of other high resolution multisensor /multispectral imageries and analytical approaches to enhance the reliability of the monitoring and prediction process of such saline land.

Acknowledgements

We would like to acknowledge the support of the Faculty of Engineering, Kumamoto University, Japan, to the first author during the completion of this research as a part of a Guest Scholar Visiting Research Fellowship.

REFERENCES

Chavez, P. S., Berlin, G. L., and Sowers, L. B., 1982. Statistical methods for selecting Landsat MSS ratios, *Journal of Applied Photographic Engineering* 8**,** 23-30.

Congalton, R., 1991. A review of assessing the accuracy of classifications of remotely sensed data. *Remote Sensing of Environment* 37, 35–46.

GRASS Development Team, 2004. http://grass.itc.it/ and http://wgrass.media.osaka-cu.ac.jp/ grassh /index.html.

Huang, C., Wylie, B., Yang, L., Homer, C., and Zylstra, G., 2002. Derivation of a tasseled cap transformation based on Landsat 7 at-satellite reflectance. *International Journal of Remote Sensing* 23 8, 1741–1748.

Huete, A. R., 1988. A soil-adjusted vegetation index (SAVI). *Remote Sensing of Environment* 25, 295–309.

Kauth, R. J. and Thomas, G. S. (1976) The Tasseled cap-a graphic description of the spectral-temporal development of agricultural crops as seen by Landsat, In: *Proceedings of remotely sensed data*, Purdure University, West Lafayette, IN, 41–57.

Landsat Project Science Office, 2002. Landsat 7 science data user's handbook. Goddard Space Flight Center (2002), http://ltpwww.gsfc.nasa.gov/IAS/handbook/handbook_toc.html .

Lunetta, R. S., Ediriwickrema, J., Johnson, D., Lyon, J.G. and McKerrow, A., 2002 Impacts of vegetation dynamics on the identification of land-cover change in a biologically complex community in North Carolina, USA. *Remote Sensing of Environment* 82, 258–270.

Markham, B. L. and Barker, J. L., 1986. Landsat MSS and TM post-calibration dynamic ranges, exoatmospheric reflectances and at-satellite temperatures. *Landsat Technical Notes* 1, 3–8.

Misak, R. F., Abdel Baki, A. A., and El-Hakim, M. S., 1997. On the causes and control of the waterlogging phenomenon, Siwa Oasis, northern Western Desert, Egypt. *Journal of Arid Environment* 37, 23-32.

Washburne, J. C., 1994. A distributed surface temperature and energy balance model of semi-arid watershed. Ph.D. Dissertation, University of Arizona, Dept. of Hydrology and Water Research. 412 p.

Wukelic, G.E., Gibbons, D.E., Martucci, L.M. and Foote, H.P., 1989. Radiometric calibration of Landsat Thematic Mapper thermal band. *Remote Sensing of Environment* 28, 339–347.

Zhan, X., Sohlberg, R.A., Townshend, R.G., DiMiceli, C., Carroll, M.L., Eastman, J.C., Hansen, M.C., and DeFries, R.S., 2002. Detection of land cover changes using MODIS 250 m data. *Remote Sensing of Environment* 83, 336–350.